Received: 7 October 2022 | Accepted: 18 October 2022

DOI: 10.1002/pamm.202200192

A comparative study between phase-field and micromorphic gradient-extended damage models for brittle fracture

Ali Harandi[1,*], **Majd Tabib**[1], **Baker Alatassi**[1], **Tim Brepols**[1], **Shahed Rezaei**[2], and **Stefanie Reese**[1]

[1] Institute of Applied Mechanics, RWTH Aachen University, Mies-van-der-Rohe-Str. 1, 52074 Aachen, Germany
[2] Mechanics of Functional Materials Division, Institute of Materials Science, Technical University of Darmstadt, Otto-Berndt-Str. 3, 64287 Darmstadt, Germany

To circumvent a mesh dependency of damage models, non-local approaches such as phase-field and gradient-extended damage models have shown a good capability and attracted a lot of attention for modeling fracture. These models can predict crack nucleation, kinking, and branching. The gradient-extended formulation proposed by [1, 2], which includes a micromorphic degree of freedom for damage, is connected to a phase-field damage model presented in [3]; by connecting fracture parameters in brittle fracture. The latter is followed by comparing the thermodynamic consistency of these models. Despite having similarities in the formulation, gradient-extended models differ from the standard phase-field ones by having a damage threshold. Besides that, the local iteration exists in the gradient-extended damage models. By employing the cohesive phase-field model or the Angiotensin type 1 (AT1), a damage threshold appears in the formulation; by having a linear term for damage in the crack density function, see [4,5,12]. A comparison between these models is made, by taking several numerical examples and comparing their responses in a quasi-static case. Moreover, the feasibility of different responses is addressed when one uses a standard Newton-Raphson solver or the arc-length one for solving a boundary value problem.

1 Introduction

Predicting cracking and fracture in solids poses a lot of problems. On the one hand, discrete fracture approaches like the extended finite element method and cohesive zone models tackle many problems see [6, 7] respectively. On the other hand, employing them imposes some pre- or peri-computation efforts see [8]. Continuum damage models don't suffer from the mentioned problem since damage enters into their formulation as a scalar [9] or tensors of different orders [10]. Employing a non-local approach by utilizing an internal length scale to prescribe the gradient effects can overcome the mesh dependency of local damage models, see [11]. Phase-field damage models also show insensitive results concerning the mesh by using a regularized crack surface energy, see [12].

The comparison has been made between gradient-extended damage models and phase-field ones in [13, 14]. The scope of the present work is to compare gradient-extended damage models that utilize a micromorphic scalar variable for damage, see [1, 2], with the standard phase-field damage models in terms of thermodynamical consistency, formulation, and in a numerical example.

This work represents the models' thermodynamically consistent formulation and shows how they can be connected together. Followed by a numerical example and discussion about their features.

2 Constitutive modeling

Gradient-extended damage model based on the micromorphic methodology (GE). The gradient-extended damage model based on a scalar micromorphic damage variable in the sense of [1, 2], is presented in this section, in the large deformation framework and for the brittle fracture behavior. The Helmholtz free energy ψ^{PF} consists of three parts: elastic stored energy ψ_e, damage hardening part ψ_d, and energy associated with the micromorphic extension $\psi_{\bar{d}}$ which is defined as

$$\psi^{\text{GE}} = f_d(d)\,\psi_e(\boldsymbol{C}) + \psi_d(d) + \psi_{\bar{d}}(d, \bar{d}, \nabla\bar{d}), \tag{1}$$

where a degradation function is defined as $f_d(d) = (1-d)^2$. In the following equations, d stands for the local damage variable while $\bar{d}$ indicates the micromorphic one. Meanwhile $\boldsymbol{C}$ represents the right Cauchy-Green deformation tensor. The Clausius-Duhem inequality for the gradient-extended damage models based on the micromorphic approach is written as

$$-\dot{\psi}^{\text{GE}} + \boldsymbol{S} \cdot \frac{1}{2}\dot{\boldsymbol{C}} + a_{0_i}\dot{\bar{d}} + \boldsymbol{b}_{0_i} \cdot \nabla\dot{\bar{d}} \geq 0. \tag{2}$$

In Eq. 2, $\boldsymbol{S}$ represents the second Piola-Kirchhoff stress tensor, and the last two terms stand for the contributions from the micromorphic damage and its gradient, respectively. After some steps, the conjugate forces are derived as

$$\boldsymbol{S} = f_d(d)\,2\,\frac{\partial\psi_e}{\partial\boldsymbol{C}}, \qquad a_{0_i} = \frac{\partial\psi_{\bar{d}}}{\partial\bar{d}}, \qquad \boldsymbol{b}_{0_i} = \frac{\partial\psi_{\bar{d}}}{\partial\nabla\bar{d}}. \tag{3}$$

* Corresponding author: e-mail ali.harandi@ifam.rwth-aachen.de, phone +49 241 80 25003, fax +49 241 80 22001

Where a_{0_i} and $\boldsymbol{b}_{0_i}$ are the generalized forces. Meanwhile, by employing a sufficiently large penalty parameter H, a_{0_i} will disappear. Finally, the remaining part of Eq. 2 becomes

$$-\left(\frac{\mathrm{d}f_d(d)}{\mathrm{d}d}\,\psi_e \,+\, \frac{\partial \psi_{\bar{d}}}{\partial d} \,+\, \frac{\partial \psi_d}{\partial d}\right)\dot{d} \,\geq\, 0. \tag{4}$$

In order to fulfill the Eq. 4 inequality, a damage surface is defined as

$$\Phi_d = Y \,-\, Y_0 \,-\, \frac{\partial \psi_d}{\partial d}, \tag{5}$$

in which $Y := -\dfrac{\mathrm{d}f_d(d)}{\mathrm{d}d}\,\psi_e - \dfrac{\partial \psi_{\bar{d}}}{\partial d}$, and Y_0 is the damage threshold and can be considered as an additional material parameter, see [2]. Finally, an evolution equation is derived as

$$\dot{d} = \dot{\lambda}_d \,\frac{\partial \Phi_d}{\partial Y} = \dot{\lambda}_d, \tag{6}$$

where the $\dot{\lambda}_d$ refers to a damage multiplier. In order to guarantee damage irreversibility, Karush-Kuhn-Tucker conditions are employed as

$$\dot{\lambda}_d \,\geq\, 0, \qquad \Phi_d \,\leq\, 0, \qquad \dot{\lambda}_d \Phi_d = 0. \tag{7}$$

One concludes that a local iteration is mandatory to solve the evolution equation for the local damage variable in the gradient-extended damage model based on the micromorphic approach.
For a compressible Neo-Hookean-type 2-D solid, one can write the elastic stored free energy as

$$\psi_e \,=\, \frac{\mu}{2}\left(\mathrm{tr}(\boldsymbol{C}) - 2 \,-\, 2\ln\left(\sqrt{\det(\boldsymbol{C})}\right)\right) \,+\, \frac{\Lambda}{4}\left(\det(\boldsymbol{C}) - 1 \,-\, 2\ln\left(\sqrt{\det(\boldsymbol{C})}\right)\right). \tag{8}$$

In which μ and Λ are the Lamé constants. The damage hardening energy and micromorphic part are defined as $\psi_d = \dfrac{1}{2}\,r d^2$ and $\psi_{\bar{d}} = \dfrac{H}{2}\left(d - \bar{d}\right)^2 \,+\, \dfrac{A}{2}\,\nabla\bar{d}\cdot\nabla\bar{d}$, respectively. In the previously mentioned equations, r and A are material parameters, and H refers to a penalty parameter that enforces the local and the micromorphic damage variables share the same value. It is worth mentioning that the above choices are arbitrary for the Helmholtz free energy of each part.
Taking into account a domain Ω, one needs to satisfy two different balances: the balance of linear momentum and a micromorphic balance. These equations, in the absence of body forces, read in the form of partial differential equations (PDE) as

$$\mathrm{Div}(\boldsymbol{F}\boldsymbol{S}) = \boldsymbol{0} \text{ in } \Omega, \qquad \mathrm{Div}(A\nabla\bar{d}) \,-\, H(d - \bar{d}) = 0 \text{ in } \Omega. \tag{9}$$

In Eq. 9, $\boldsymbol{F}$ denotes to the deformation gradient. The model inherits an internal length scale which can be computed as $l_c = \sqrt{\dfrac{A}{H}}$, and a boundary condition needs to be satisfied additionally as $\nabla\bar{d}\cdot\boldsymbol{n} = 0$ on Γ, where $\boldsymbol{n}$ is the normal vector on the boundary Γ.

Angiotensin type 2 (AT2) phase-field damage model (PF). The phase-field damage model is a regularized formulation of Griffith's brittle fracture, see [3]. That substitutes a strong discontinuity (crack) with a diffuse one. One can write the crack-free energy of the AT2 phase-field damage model ψ_c as

$$\psi_c = G_c\,\left(\frac{1}{2\,l_c}\,\bar{d}^{\,2} \,+\, \frac{l_c}{2}\,\nabla\bar{d}\cdot\nabla\bar{d}\right). \tag{10}$$

In Eq. 10, $\bar{d}$ stands for the phase-field variable (damage), G_c is the fracture energy, and l_c is the internal length scale. The Helmholtz free energy of the system is written as

$$\psi^{\mathrm{PF}} \,= f_d(\bar{d})\,\psi_e(\boldsymbol{C}) \,+\, \psi_c(\bar{d}). \tag{11}$$

Similarly to gradient-extended damage models, once again, we start from the Clausius-Duhem inequality as

$$\int_R \left(-\dot{\psi}^{\mathrm{PF}} \,+\, \boldsymbol{S}\cdot\frac{1}{2}\,\dot{\boldsymbol{C}} \,+\, \boldsymbol{\xi}\cdot\nabla\dot{\bar{d}} \,-\, \pi\dot{\bar{d}}\right) dR \,\geq\, 0. \tag{12}$$

Please note that for utilizing the divergence theorem in simplifying the inequality, one needs to use an integral form and consider a micro part of the body as depicted in Fig. 1.

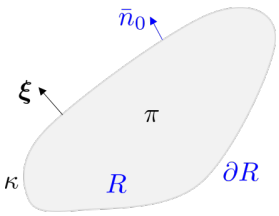

$\boldsymbol{\xi}$: micro-stresses
π: internal micro-force
κ: external micro-force

Fig. 1: The micro part of a body with having micro-stresses and micro-forces.

Contrary to gradient-extended damage models, the micro-force balance is utilized directly to derive conjugate forces and simplify the inequality as $\mathrm{Div}(\boldsymbol{\xi}) + \pi + \kappa = 0$. Analogously to Eq. 3, the second Piola-Kirchhoff stress tensor is derived as $\boldsymbol{S} = f_d(\bar{d})\, 2\, \dfrac{\partial \psi_e}{\partial \boldsymbol{C}}$, and micro-stresses are $\boldsymbol{\xi} = \dfrac{\partial \psi_c}{\partial \nabla \bar{d}}$ which is identical to $\boldsymbol{b}_{0_i}$. The remaining part of inequality in Eq. 12, after performing divergence theorem and neglecting the external micro-force reads

$$\left(\frac{\partial \psi^{\mathrm{PF}}}{\partial \bar{d}} - \mathrm{Div}\left(\frac{\partial \psi^{\mathrm{PF}}}{\partial \nabla \bar{d}} \right) \right) \dot{\bar{d}} \geq 0. \tag{13}$$

For satisfying the Eq. 13, according to [15], an evolution equation is derived as

$$\dot{\bar{d}} = -M \left(\frac{\partial \psi^{\mathrm{PF}}}{\partial \bar{d}} - \mathrm{Div}\left(\frac{\partial \psi^{\mathrm{PF}}}{\partial \nabla \bar{d}} \right) \right). \tag{14}$$

In Eq. 14, M represents the mobility term, and in the quasi-static case, one can assume $M \to \infty$. By considering the domain Ω, the latter enforces another PDE, the balance of dissipated energy, which has to be solved in addition to the balance of linear momentum as

$$\mathrm{Div}(\boldsymbol{F}\boldsymbol{S}) = \boldsymbol{0} \text{ in } \Omega, \qquad \left(\frac{\partial \psi^{\mathrm{PF}}}{\partial \bar{d}} - \mathrm{Div}\left(\frac{\partial \psi^{\mathrm{PF}}}{\partial \nabla \bar{d}} \right) \right) = 0 \text{ in } \Omega. \tag{15}$$

Consequently, there is no additional local evolution equation in phase-field damage models. For completeness, damage irreversibility cannot be guaranteed by only satisfying the balance of dissipated energy. That leads to using history variables for damage or the elastic stored energy ψ_e in order to use the maximum amount of stored energy as a damage driving force. In this work, we have chosen the second option; see [3] for more details.
The elastic stored energy has been chosen the same as the gradient-damage part. The same also for the degradation function of phase-field model, and we employed the $f_d(\bar{d}) = (1-\bar{d})^2$ form.

Comparison between gradient-extended and phase-field damage models by neglecting the local damage quantity in gradient-extended damage models. To compare model, the local damage part and its damage hardening-related part are removed from the GE formulation in this part. After performing some steps, one can derive the same evolution equation and system of equations as PF. In this case, the AT2 PF model can be seen as a particular type of GE model.

Table 1: Comparison of GE and PF by neglecting the local damage quantity in GE.

GE	AT2 PF	Connection
$\psi^{\mathrm{GE}} = f_d(\bar{d})\psi_e + \psi_{\bar{d}}$	$\psi^{\mathrm{PF}} = f_d(\bar{d})\psi_e + \psi_c$	identical ψ_e and f_d
$\psi_{\bar{d}} = \dfrac{H}{2}\bar{d}^2 + \dfrac{A}{2}\nabla\bar{d}\cdot\nabla\bar{d}$	$\psi_c = G_c\left(\dfrac{1}{2\,l_c}\bar{d}^2 + \dfrac{l_c}{2}\nabla\bar{d}\cdot\nabla\bar{d}\right)$	$H = \dfrac{G_c}{l_c}$ $A = G_c l_c$

Tab. 1 connects the GE material parameters to the AT2 PF ones. Under Tab. 1 assumptions, the two models are identical (AT2 PF, a particular case of GE).

Comparison between gradient-extended and phase-field damage models without neglecting the local damage quantity in gradient-extended damage models. With a sufficiently large value for the penalty parameter H, the metamorphic damage variable takes the same value as the local one ($d \approx \bar{d}$). The latter enables us to connect other terms in the two formulations and make equivalent free energies in GE and PF models by substituting d with $\bar{d}$. After some steps, the following table is derived for connecting the models' material parameters.

Table 2: Comparison of GE and PF without neglecting the local damage quantity in GE.

GE	AT2 PF	Connection
$\psi^{\text{GE}} = f_d(d)\psi_e + \psi_{\bar{d}}$	$\psi^{\text{PF}} = f_d(\bar{d})\psi_e + \psi_c$	identical ψ_e and f_d
$\psi_{\bar{d}} = \frac{A}{2}\nabla\bar{d}\cdot\nabla\bar{d}$	$\psi_c = G_c\left(\frac{1}{2\,l_c}\bar{d}^2 + \frac{l_c}{2}\nabla\bar{d}\cdot\nabla\bar{d}\right)$	$r = \frac{G_c}{l_c}$
$\psi_d = \frac{1}{2}r\bar{d}^2$		$A = G_c l_c$
		$H \to \infty$

In Tab. 2, some terms vanished resulted from the fact that the relation has been assumed.
Finally, the damage threshold Y_0 can be set to zero since, for the PF formulation, the threshold does not exist. One can refer to the cohesive phase-field formulations see [4,5], or the work of [16] in order to incorporate damage threshold in the phase-field formulation. In the scope of this work, $Y_0 \approx 0$ is considered.
Moreover, the first comparison leads to an identical formulation of phase-field. That is why we consider only the connection of formulation without neglecting the local damage quantity.

3 A numerical example: an asymmetrically notched specimen

With the formulations' connection in hand, the following asymmetrical numerical example is utilized in order to see the models' results (damage contours, and load-displacement curves). Fig. 2 shows boundary conditions and dimensions of this example.

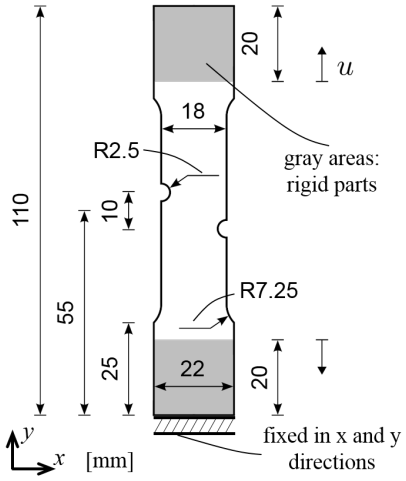

Fig. 2: Geometry and boundary conditions for a asymmetrically notched specimen.

Table 3: Material parameters for elasticity AT2 PF and GE.

elasticity:	$\Lambda = 25000$	MPa
	$\mu = 55000$	MPa
AT2 PF	$G_c = 35, 50, 70$	MPa mm
	$l_c = 5, 7$	mm
GE	$A = 250, 500$	MPa mm^2
	$r = 5, 10$	MPa
	$H = 10^6$	MPa
	$Y_0 \approx 0$	MPa

In Fig. 2, gray areas represent rigid body parts that undergo the same deformations. Tab. 3 shows the material parameters for different formulations. Please note that the elasticity parameters are the same between the two models.
Note: H is the penalty parameter and can be treated as a numerical parameter; rather than a material one. Meanwhile, a similar quantity to Y_0 is needed in PF to impose the damage threshold.
The following damage contours are obtained in Fig. 3a and Fig. 3b. Fig. 3c shows the force-displacement curve for a set of connected material parameters of two models.
For both cases, the arc-length method is utilized to solve the system of equations. To this end, the snap-back behavior is visible in Fig. 3c and Fig. 4.
Solving the system of equations without using the arc-length method, leads to a sudden drop in the force-displacement curve; see [5] for more details.

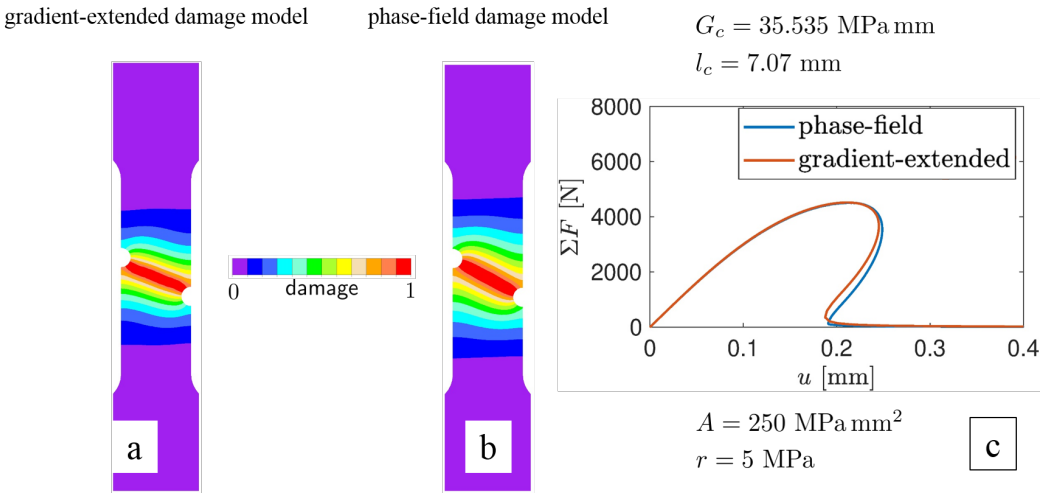

Fig. 3: a) Damage contour for the GE model. b) Damage contour for the PF model. c) Force-displacement curve for the given set of material parameters.

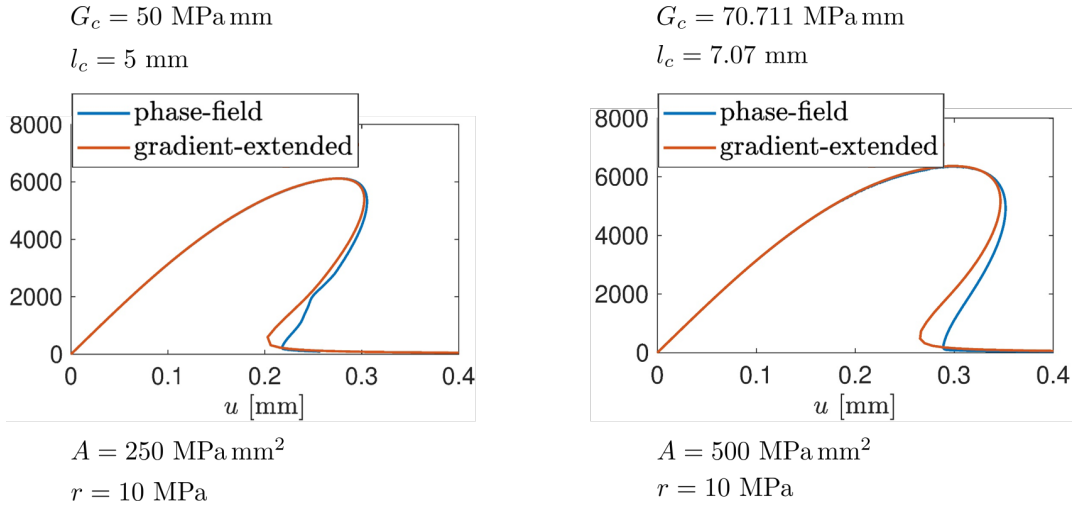

Fig. 4: Force-displacement curves for two different sets of material parameters

Models are sharing the same path until the softening regime. The deviation of gradient-extended from phase-field in a softening regime damage model can be induced by the damage threshold, despite setting it close to zero. That also leads to a smaller damage zone in gradient-extended damage models. If one puts Y_0 exactly as 0, it will trigger some numerical problems and make the simulation almost impossible. The other reason may be assuming $d = \bar{d}$. However, one should remember that these values will be sufficiently close together and are not equal since $H \to \infty$.

4 Conclusions and outlook

In this study, gradient-extended damage models based on the micromorphic approach are compared to AT2 phase-field damage models. It has been shown that both models are thermodynamically consistent, and they employ a balance of micro-forces to satisfy Clausius-Duhem inequality. Furthermore, the models' material parameters are connected. The study uses an asymmetrically notched specimen to compare the results for three different sets of parameters. Although phase-field damage models benefit from having no local evolution equation involved in the formulation, gradient-extended damage models show more flexibility for defining various damage hardening terms and different damage surfaces. All in all, the responses of these models show many similarities.

In future works, the authors aim to compare the cohesive phase-field formulation with the current gradient-extended damage model by including cohesive softening law in GE formulation. Another appealing point would be to evaluate these models, also from in terms of their compuational cost.

Acknowledgements Financial support of Subproject A6 of the Transregional Collaborative Research Center SFB/TRR 87 by the German Research Foundation (DFG) is gratefully acknowledged. Open access funding enabled and organized by Projekt DEAL.

References

[1] S. Forest, Proc. R. Soc. A **472**, 20150755 (2016).
[2] T. Brepols, S. Wulfinghoff, and S. Reese, Int. J. Plast. **129**, 102635 (2020).
[3] C. Miehe, M. Hofacker, and F. Welschinger, Comput. Methods in Appl. Mech. Eng. **199**(45-48), 2765-2778 (2010).
[4] J.-Y. Wu, and V. P. Nguyen, J. Mech. Phys. Solids **119**, 20-42 (2018).
[5] S. Rezaei, A. Harandi, T. Brepols, and S. Reese, Eng. Frac. Mech. **261**, 108177 (2022).
[6] T. Belytschko, and T. Black, Int. J. Numer. Meth. Eng. **45**(5), 601-620 (1999).
[7] S. Rezaei, S. Wulfinghoff, and S. Reese, Int. J. Solids Struct. **121**, 62-74 (2017).
[8] HR. Bayat, S. Rezaei, A. Rajaei Harandi, T. Brepols, and S. Reese, Proc. Appl. Math. Mech. **20**, e202000110 (2021).
[9] P. Maimí, P. P. Camanho, J. A. Mayugo, and C. G. Dávila, Mech. Mater. **39**(10), 897-908 (2007).
[10] S. Reese, T. Brepols, M. Fassin, L. Poggenpohl, and S. Wulfinghoff, J. Mech. Phys. Solids **146**, 104174 (2021).
[11] B. J. Dimitrijevic and K. Hackl, Int. J. Numer. Method. Biomed. Eng. **27**, 1199–1210 (2011).
[12] E. Tanné, T. Li, B. Bourdin, J.-J. Marigo, and C. Maurini, J. Mech. Phys. Solids **110**, 80-99 (2018).
[13] R. Borst, and C. Verhossel, Comput. Methods in Appl. Mech. Eng. **312**, 78-94 (2016).
[14] S. Forest, K. Ammar, and B. Appolaire, Lect. Notes Appl. Comput. Mech. **59**, 69-88 (2011).
[15] C. Kuhn, and R. Müller, Eng. Frac. Mech. **77**(18), 3625-3634 (2010).
[16] C. Miehe, M. Hoacker, L.-M Schänzel, and F. Aldakheel, Comput. Methods in Appl. Mech. Eng. **294**, 486-522 (2015).

